Identification of the *Phytophthora* PAMP Pep-13 Receptor Using Diploid Potato Inbred Lines

Xuefeng Fan[1#], Dongyue Li[1#], Lin Cheng[2#], Yuqi Zhu[1,3], Yue Han[1], Tongjun Sun[1*].

[1] Shenzhen Branch, Guangdong Laboratory for Lingnan Modern Agriculture, Genome Analysis Laboratory of the Ministry of Agriculture and Rural Affairs, Agricultural Genomics Institute at Shenzhen, Chinese Academy of Agricultural Sciences, Shenzhen, China.

[2] National Key Laboratory of Tropical Crop Breeding, Shenzhen Branch, Guangdong Laboratory of Lingnan Modern Agriculture, Genome Analysis Laboratory of the Ministry of Agriculture and Rural Affairs, Agricultural Genomics Institute at Shenzhen, Chinese Academy of Agricultural Sciences, Shenzhen, China.

[3] State Key Laboratory of Crop Stress Adaptation and Improvement, The Zhongzhou Laboratory for Integrative Biology, School of Life Sciences, Henan University, Kaifeng, China.

[#] Contributed equally.

* Correspondence: Tongjun Sun (suntongjun@caas.cn).

ABSTRACT

Plants employ cell surface receptors to recognize pathogen-associated molecular patterns (PAMPs) and activate pattern-triggered immunity, a crucial defense mechanism against invading pathogens. Pep-13 is a PAMP derived from a class of conserved cell wall transglutaminases present in *Phytophthora* species, and its receptor PERU (Pep-13 receptor unit), was reported recently. In our parallel study, we observed distinct responses to Pep-13 between two diploid potato inbred lines: E4-63 recognizes Pep-13, whereas A6-10 does not. Genetic analysis demonstrated that Pep-13 recognition in E4-63 is controlled by a single genetic locus, tentatively designated *TGER* (*Transglutaminase elicitor response*). Through bulked segregant analysis sequencing, followed by complementation assays, we found that the *TGERa* gene in E4-63 is essential for Pep-13 recognition. Sequence alignment revealed that TGERa shares 99.91% amino acid sequence identity with PERU, indicating that *TGERa* and *PERU* are allelic variants of the same gene (*PERU*/*TGERa*). *TGERb*, a highly homologous gene of *TGERa*, was identified in the E4-63 genome; notably, TGERa, but not TGERb, can recognize Pep-13. We further demonstrated that TGERb exhibits defects in both ligand binding and association with the co-receptor StSERK3A. Additionally, we found that the *TGERa* allele in A6-10 is a weak allele with reduced expression levels, presumably resulting from a 3 kb DNA fragment insertion in its first intron. Heterologous introduction of *TGERa* into *Nicotiana benthamiana* and tomato significantly enhanced their resistance to *Phytophthora infestans*. Collectively, our findings confirm that PERU/TGERa functions as the Pep-13 receptor in potato and provide a valuable molecular target for improving *Phytophthora* resistance in plants.

Keywords: Potato; *Phytophthora infestans*; Pep-13; Pattern Recognition Receptor (PRR); PERU/TGERa.

INTRODUCTION

Potato (*Solanum tuberosum* L.), the most important tuber crop, is a staple food for approximately 1.3 billion people globally (Stokstad, 2019). Cultivated potatoes are primarily propagated asexually via tubers, and the complexity of their tetraploid genome results in a prolonged breeding cycle. To address this challenge, a diploid potato hybrid breeding project was launched based on diploid potato inbred lines (Zhang et al., 2021; Cheng et al., 2025), which not only accelerates the potato breeding process but also provides materials and genomic data resources for research on potato functional genomics.

Late blight, caused by *Phytophthora infestans*, is a devastating disease affecting potato yield (Nowicki et al., 2012), and harnessing the plant's own immune receptors provides a sustainable and eco-friendly solution for late blight control. Specifically, pattern recognition receptors (PRRs) localized on the plant cell surface recognize pathogen-associated molecular patterns (PAMPs), thereby initiating pattern-triggered immunity that restricts pathogen invasion (Jones and Dangl, 2006; Zhou and Zhang, 2020). A few well-studied PAMPs have been reported in the genus *Phytophthora*, such as INF1, nlp20, and XEG1, which are specifically recognized by ELR (Du et al., 2015) and NbREL (Chen et al., 2023a), *Arabidopsis* RLP23 (Albert et al., 2015), and NbRXEG1 (Wang et al., 2018), respectively. Notably, heterologous expression of such PRRs confers enhanced disease resistance in plants (Albert et al., 2015; Chen et al., 2023a).

Pep-13 is a 13-amino-acid peptide derived from a class of cell wall transglutaminases (TGase) in the genus *Phytophthora*, and Pep-25 is a 25-amino-acid peptide that contains the Pep-13 sequence (Nürnberger et al., 1994). Both peptides share similar activity: perception of Pep-13/25 by potato triggers immune responses including MAPK activation, ROS burst, upregulation of defence genes, and the induction of hypersensitive cell death (Nürnberger et al., 1994; Brunner et al., 2002). However, the receptor for Pep-13 remained unknown for a long time until recently. PERU, a typical

79 leucine-rich repeat receptor kinase (LRR-RK), was identified as the receptor of
80 Pep-13 from potato *cv.* DM (Torres Ascurra et al., 2023). Interestingly, PERU
81 from accession LPH680-5 ($PERU^{LPH}$) was shown to have a broad recognition
82 ability that perceives Pep-13/25 and Pep-25 variants, including the nearly
83 inactive Pep-25W2A (Torres Ascurra et al., 2023).
84 In our parallel study, we explored the Pep-13-triggered response in the inbred
85 lines A6-10, A6-26 and E4-63, which are the parent lines for hybrid potatoes
86 (Zhang et al., 2021). We found that Pep-13 triggered hypersensitive cell death
87 in A6-26, E4-63 and Hybrid 2 (a F_1 progeny of a cross between A6-10 and
88 E4-63), but not in A6-10 (Supplemental Figure 1A). Meanwhile, the F_2
89 population derived from self-pollinated Hybrid 2 showed phenotypic
90 segregation in response to Pep-13, with the ratio of Pep-13-responsive (HR)
91 plants to non-responsive (non-HR) plants being approximately 3:1
92 (Supplemental Figure 1B); this result indicates that Pep-13 recognition in
93 E4-63 is controlled by a single genetic locus, which we tentatively designated
94 *TGER* (*Transglutaminase elicitor response*). However, conflicting with this
95 finding, the research on PERU indicated that there are no PERU homologs in
96 A6-26 and E4-63 (See Supplemental data_s4 of Torres Ascurra et al., 2023).
97 In this study, we identified that *TGERa* in E4-63 is essential for Pep-13
98 recognition. Sequence alignment revealed that TGERa shares 99.91% amino
99 acid identity with PERU, indicating that *TGERa* and *PERU* are the same gene
100 (designated as *PERU*/*TGERa*; for simplicity, *TGERa* is used hereafter). We
101 further identified *TGERb*, a highly homologous gene of *TGERa* in the E4-63
102 genome, which cannot recognize Pep-13. Additionally, we found that the
103 *TGERa* allele in A6-10 is a weak allele with reduced expression. Lastly, we
104 showed that introduction of *TGERa* into plants significantly enhanced their
105 resistance to *Phytophthora* pathogens, highlighting the potential of *TGERa* as
106 a valuable molecular target for improving *Phytophthora* resistance in crops.
107

RESULTS AND DISCUSSION

Differential responses of potato inbred lines A6-10, A6-26 and E4-63 to Pep-13

To identify the receptor responsible for Pep-13 perception using potato inbred lines generated by the Upotato project (Zhang et al., 2021), we first evaluated their responses to Pep-13. As shown in Figure 1A, A6-26 and E4-63 exhibited hypersensitive response (HR) cell death to Pep-13 but not to the nearly inactive Pep-13W2A variant (Brunner et al., 2002). Unexpectedly, Pep-13 failed to trigger cell death in A6-10, although A6-10 and A6-26 are homozygous inbred lines derived from the same ancestral parent, PG6359 (Zhang et al., 2021). Additionally, Désirée, but not the Atlantic, exhibited cell necrosis upon Pep-13 treatment (Figure 1A). Consistent with the HR phenotypes, Pep-13 treatment activated MAPK signaling in A6-26 but not in A6-10 (Figure 1B and 1C). Notably, four Pep-13-responsive genes (Nietzschmann et al., 2019), namely *StTHT*, *StPALs*, *StFAD*, and *St4-CL*, were strongly induced in A6-26, but showed little or no induction in A6-10 (Figure 1D). Collectively, these results demonstrate distinct responses of potato lines to Pep-13, with A6-10 showing a unique pattern of no cell death but weak induction of some Pep-13-responsive genes.

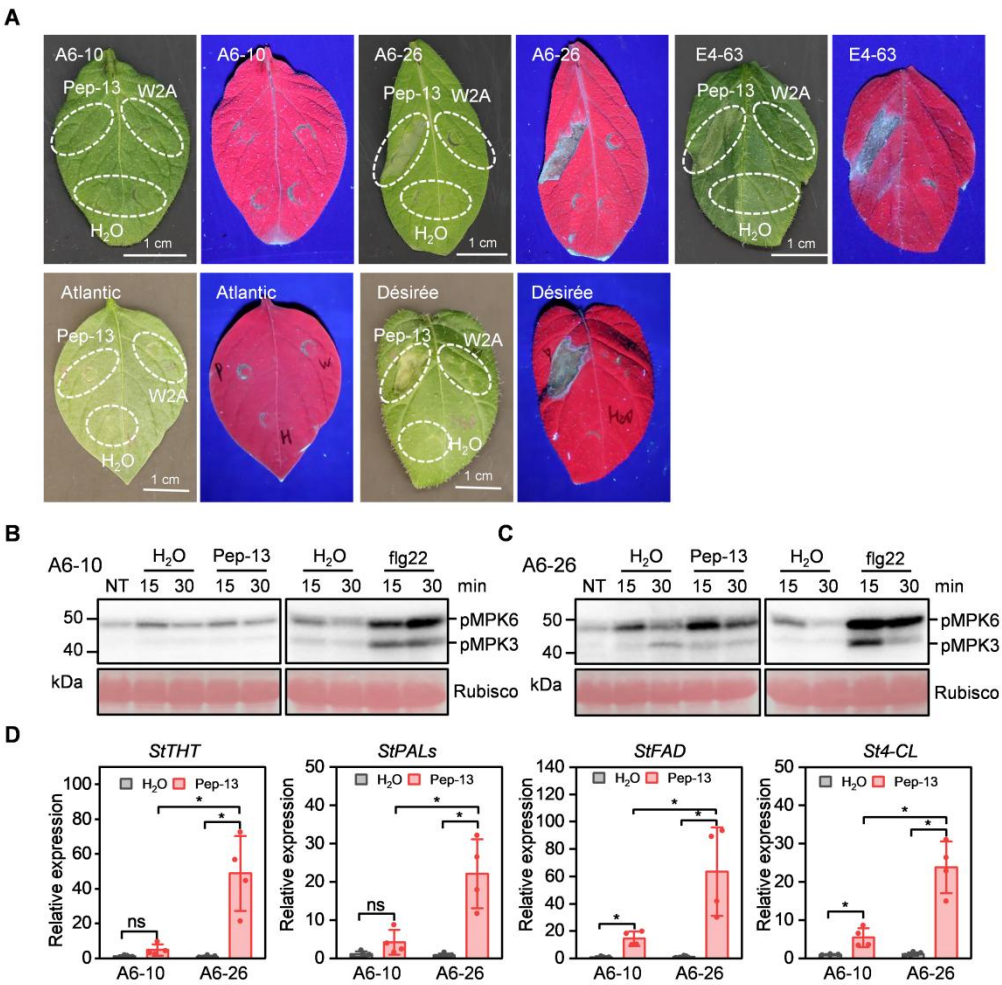

Figure 1. Differential responses of potato inbred lines A6-10, A6-26, E4-63 and cultivars Atlantic and Désirée to Pep-13.

(A) Differential responses of potato cultivars to Pep-13. Leaves were infiltrated with 100 μM Pep-13, Pep-13W2A (a Pep-13 variant) and H_2O. Photos were taken under natural light (green leaf) and UV light (red fluorescence) at 24 h post-infiltration. Bar = 1 cm.

(B-C) Pep-13-induces MAPK activation in A6-26 but not in A6-10. Leaves of A6-10 **(B)** and A6-26 **(C)** were sprayed with 100 μM Pep-13 or H_2O. Samples were collected at 15 and 30 min post-treatment, and MAPK activation was detected by western blot using an anti-p44/42-ERK antibody. flg22 (5 μM) served as a positive control, and non-treated (NT) leaves served as a negative control.

(D) Pep-13-responsive genes are strongly induced in A6-26 but show little or no induction in A6-10. Transcript levels of *StTHT*, *StPALs*, *StFAD*, and *St4-CL* were analyzed by RT-qPCR in leaves of A6-10 and A6-26 at 4 h after infiltration with 100 μM Pep-13 or H_2O. *NbEF1α* used as reference gene. Data represent mean ± s.d. n = 4. Asterisks indicate statistically significant differences (*$p < 0.05$, Student's t-test); ns, no significant difference.

Genetic mapping of *TGERa* and validation

Using bulked segregant sequencing, we identified that the *TGER* locus is located within the chromosome 3:0-3 Mb region of the E4-63 genome, which

147 was further narrowed down to 24 candidate genes (see details in
148 Supplemental Note 1). We successfully cloned 21 of these candidate genes
149 and screened their responsiveness to Pep-13 via *Agrobacterium*-mediated
150 transient expression in *N. benthamiana* (*Nb*) leaves. The gene expressed by
151 construct #9 was found to respond to Pep-13 (Supplemental Figure 2), which
152 was designated as *TGERa*. Next, we generated transgenic *Nb* lines
153 expressing *TGERa* under its native promoter (*np-TGERa Nb* lines); these
154 transgenic lines exhibited cell death in response to Pep-25 but showed no or
155 weak cell death to Pep-13 treatment (Supplemental Figure 3A). However, both
156 Pep-13 and Pep-25 were able to induce MAPK activation in *np-TGERa Nb*
157 lines; furthermore, Pep-13 treatment of these transgenic plants significantly
158 activated the expression of *NbACRE31* and *NbCYP71D20* (Supplemental
159 Figure 3B and 3C). These results indicate that *TGERa* is responsive to both
160 Pep-13 and Pep-25, with Pep-25 exhibiting stronger activity in inducing cell
161 death than Pep-13 under conditions of low TGERa protein levels. Stable
162 expression of *TGERa* in cv. MicroTOM and potato Atlantic conferred the ability
163 to recognize Pep-13 and Pep-25, leading to the induction of cell death
164 (Supplemental Figure 3D-3G). Collectively, these findings demonstrated that
165 TGERa is responsive to Pep-13/25.

166 **Immune-related SERKs are required for Pep-13 perception**

167 TGERa is a typical leucine-rich repeat receptor kinase (LRR-RK). To identify its
168 interacting proteins, immunoprecipitation-mass spectrometry (IP-MS) was
169 performed in *N.benthamiana* (*Nb*) leaves, revealing six NbSERK proteins,
170 including NbSERK3A, NbSERK3B, NbBAK1a, NbBAK1b, NbSERK2a, and
171 NbSERK2b, as Pep-13-induced interacting partners of TGERa (Supplemental
172 Figure 4A). Phylogenetic analysis showed that these six NbSERK proteins,
173 together with their potato homologs (StSERK2, StSERK3A, and StSERK3B)
174 and *Arabidopsis* SERKs (Ma et al., 2016; Li et al., 2025), form a single clade
175 (Supplemental Figure 4B). Given the evolutionary conservation of these SERK
176 proteins and their known roles in plant immunity, we further confirmed that

177 Pep-13 induces the interaction between TGERa and three StSERKs
178 (Supplemental Figure 5A-5C). Additionally, silencing of these six *NbSERK*
179 genes in *Nb* leaves blocked Pep-25/TGERa-induced cell death (Supplemental
180 Figure 5D-5J). Notably, we showed that TGERa can bind to biotin-labeled
181 Pep-13 (Supplemental Figure 5L). Collectively, these results demonstrate that
182 TGERa forms a receptor complex with immune-related SERKs to mediate the
183 perception of Pep-13.

184 **Comparison of coding sequences between TGERa and PERU**

185 Sequence analysis revealed that the coding sequence (CDS) of TGERa^{E4-63} is
186 78 bp longer than that of PERU^{DM}, which corresponds to an in-frame upstream
187 open reading frame (uORF) (Supplemental Figure 6A). This observation
188 indicates that the predicted TGERa^{E4-63} contains an additional 26 amino acids
189 at the N-terminus compared to PERU^{DM}; whereas the remaining protein
190 sequence is nearly identical between the two, with only a single amino acid
191 substitution (A317 in PERU vs. G317 in TGERa-dN26), confirming that
192 TGERa^{E4-63} and PERU^{DM} are allelic variants of the same gene.

193 To determine the translational start site of TGERa^{E4-63}, we individually mutated
194 the ATG codons of uORF1 and the main ORF. Mutation of the main ORF ATG,
195 which restricts protein translation to uORF1, significantly reduced TGERa^{E4-63}
196 protein accumulation irrespective of being driven by CaMV 35S or its native
197 promoters (Supplemental Figure 6B-6E). These findings indicate that
198 TGERa^{E4-63} protein translation primarily initiates from the main ATG. Given that
199 TGERa is a single-pass transmembrane protein, the additional 26-amino-acid
200 sequence at the N-terminus may impair its signal peptide function and disrupt
201 biosynthetic process of TGERa^{E4-63} protein, thereby reducing its protein
202 stability.

203 In contrast, the annotated PERU protein from LPH60-5 (PERU^{LPH}) contains an
204 extra 24-amino-acid sequence between residues T372 and G373 compared to
205 TGERa/PERU, which is encoded by the in-frame intron 2 (Supplemental
206 Figure 7A and 7B). Further analysis demonstrated that this intron 2 retention

207 occurs in a subset of *TGERa* transcripts extracted from A6-26 leaves, both
208 under normal conditions and following *Phytophthora* inoculation (Supplemental
209 Figure 7C and 7D). To characterize the function of the protein translated from
210 transcripts with intron 2 retention, we introduced synonymous mutations into
211 this intron 2 to generate *TGERa-In2R*, which abolishes intron 2 splicing while
212 preserving the encoded sequence as the extra 24 amino acids in PERU^{LPH}
213 (Supplemental Figure 7E and 7F). Functional assays showed that, in contrast
214 to TGERa, TGERa-In2R failed to activate MAPK or induce cell death following
215 Pep-13 treatment (Supplemental Figure 8A and 8B) and was unable to bind
216 Pep-13 or Pep-25 (Supplemental Figure 8C and 8D). These results
217 demonstrate that the protein translated from transcripts with the intron 2
218 retention is non-functional. Therefore, the additional sequence in PERU^{LPH} is
219 likely attributable to annotation errors and is unrelated to its broad ligand
220 recognition ability.

221 **TGERa/PERU, but not its close homolog TGERb, recognizes Pep-13**

222 Sequence alignment between the gene present in construct #9 and the target
223 gene *E454_03G001350.1* revealed multiple single nucleotide polymorphisms
224 (SNPs) and one insertion/deletion (indel) (Supplemental Table 3). A sequence
225 identical to *E454_03G001350.1* was subsequently re-isolated from the
226 amplification products using the same primers for *E454_03G001350.1* and
227 designated as *TGERb*. Transient expression of *TGERa,* but not *TGERb*, in
228 *N.benthamiana* (*Nb*) leaves triggered MAPK activation and cell death following
229 Pep-13 treatment (Supplemental Figure 9A and 9B). Consistently, Pep-25
230 treatment induced cell death in transgenic *Nb* lines expressing *TGERa* but not
231 in lines expressing *TGERb* (Figure 2A). In addition, *np-TGERb Nb* lines failed
232 to elicit reactive oxygen species (ROS) burst or MAPK activation following
233 Pep-13 treatment (Figure 2B, 2C, and Supplemental Figure 9C). Further
234 biochemical analyses showed that Pep-13 treatment did not promote the
235 interaction between *TGERb* and StSERK3A (Figure 2D). In contrast to TGERa,
236 TGERb was unable to bind either Pep-13 or Pep-25 (Figure 2E and 2F).

Collectively, these results demonstrated that TGERb can not recognize Pep-13 or Pep-25, highlighting a functional divergence between the two highly homologous proteins.

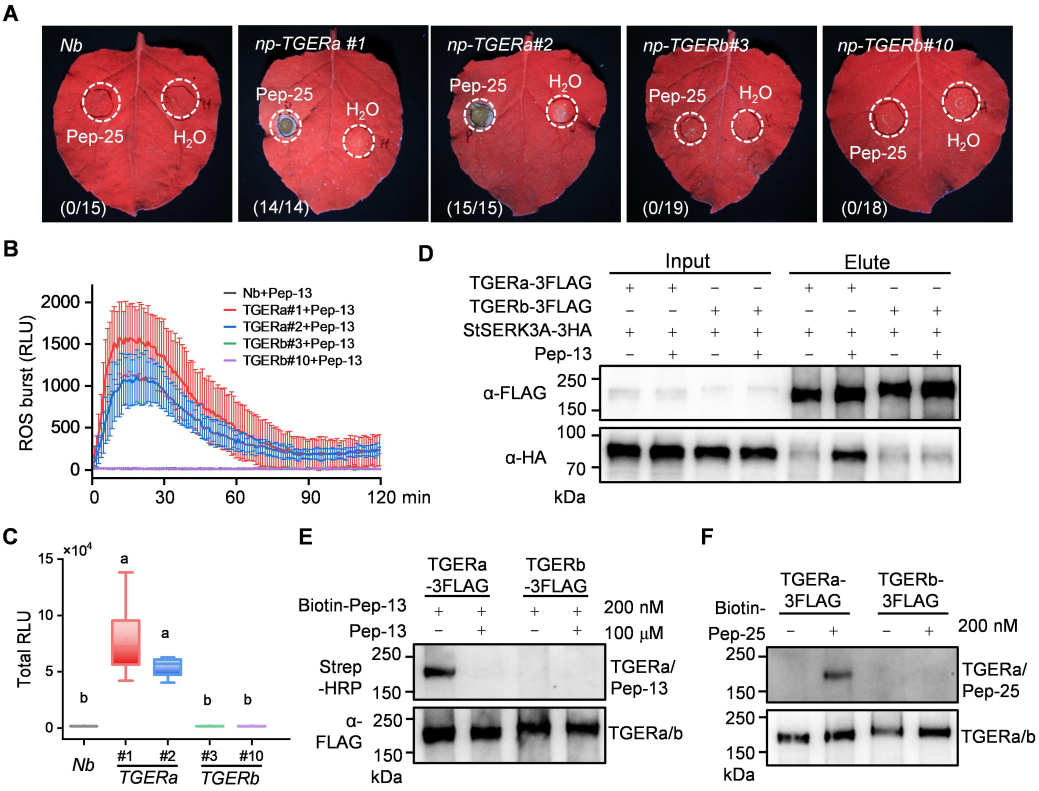

Figure 2. TGERa/PERU, but not its close homolog TGERb, recognizes Pep-13.

(A) Pep-25-induced cell death in transgenic *N. benthamiana* (*Nb*) lines expressing *TGERa* but not *TGERb.* Leaves of transgenic lines *np-TGERa* #1, *np-TGERa* #2, *np-TGERb* #3, and *np-TGERb* #10 (driven by their native promoters) were infiltrated with 100 μM Pep-25. *Nb* plants served as a negative control. Photographs were taken under UV light 5 days after infiltration.

(B-C) Pep-13-induced ROS burst in transgenic lines *np-TGERa* #1 and #2, but not in transgenic lines *np-TGERb* #3 and #10, as shown by the ROS burst curves **(B)** and total ROS production **(C)** induced by 100 nM Pep-13. Data was analyzed by two-way ANOVA followed by Tukey's multiple comparison test. Different letters indicate significant differences ($p < 0.05$, n = 8).

(D) TGERa, but not TGERb, associates with the co-receptor StSERK3A upon Pep-13 treatment. *TGERa-3Flag* or *TGERb-3Flag* was transiently co-expressed with *StSERK3A-3HA* in *Nb* leaves mediated by *Agrobacterium*. After 24 h, leaves were infiltrated with 100 μM Pep-13 or H_2O. Samples were collected 15 min post-infiltration, and TGERa/b-3Flag proteins were enriched using M2 beads. IP eluates were analyzed by western blot using anti-Flag and anti-HA antibodies.

(E-F) TGERa, but not TGERb, binds biotin-labeled Pep-13 **(E)** and Pep-25 **(F)**. *TGERa-3Flag* and *TGERb-3Flag* were transiently expressed in *Nb* leaves for 24 h. Leaves were co-infiltrated with 200 nM biotin-Pep-13/25 and 3 mM EGS, then incubated for 30 min at room temperature.

261 Excess unlabeled Pep-13 (100 μM) was included as a competitor. TGERa/b-3Flag proteins
262 were enriched using M2 beads, and IP eluates were detected by western blot using an
263 anti-Flag antibody and Strep-HRP.
264

265 **TGERb exhibits defects in both ligand binding and association with**
266 **StSERK3A**

267 Protein sequence analysis revealed that the differences between TGERa and
268 TGERb are primarily inside their ectodomains, which share 85.3% sequence
269 identity (Supplemental Figure 9D). Domain swapping experiments further
270 confirmed that divergence in the ectodomain is responsible for the inability of
271 TGERb to perceive Pep-13 (Supplemental Figure 9E and 9F).
272 The ectodomain of TGERa contains 27 leucine-rich repeats (LRRs), whereas
273 TGERb harbors an additional 24-amino acid insertion in the region
274 corresponding to LRR24 of TGERa, resulting in a total of 28 LRRs. A TGERa
275 variant carrying this additional sequence (TGERa^{b24aa}) retained the ability to
276 recognize Pep-13 (Supplemental Figure 9G and 9H), indicating that this extra
277 peptide does not affect TGERa function.
278 To elucidate the mechanism underlying TGERb's inability to recognize pep-13,
279 we first performed *in silico* LRR substitution and predicted the interface
280 predicted TM-score (ipTM) values between chimeric TGERa variants and
281 Pep-13 using AlphaFold3 (Supplemental Table 4). Based on these predictions,
282 six LRRs from TGERb (LRR5/7/9/10/17/21) were selected for function analysis.
283 Among them, LRR5, LRR7, LRR9, and LRR10 were predicted to contribute to
284 Pep-13 binding, whereas LRR17 and LRR21 were hypothesized to modulate
285 interactions with SERKs. Each of these LRRs was individually substituted into
286 TGERa (Figure 3A). Functional assays revealed that TGERa^{LRR5b} and
287 TGERa^{LRR7b} exhibited impairment in Pep-13-induced cell death and ROS burst,
288 whereas TGERa^{LRR9b}, TGERa^{LRR10b}, and TGERa^{LRR17b} completely lost
289 responsiveness to Pep-13. In contrast, TGERa^{LRR21b} retained normal Pep-13
290 responsiveness (Figure 3B and 3C). Ligand-binding assays further showed
291 that TGERa^{LRR5b} and TGERa^{LRR7b} had reduced Pep-13 binding capacity, while

TGERa^{LRR9b} and TGERa^{LRR10b} failed to bind Pep-13. Surprisingly, TGERa^{LRR17b}, similar to TGERa^{LRR21b}, retained the ability to bind Pep-13 (Figure 3D). Given that TGERa^{LRR17b} retained Pep-13 binding but failed to trigger immune responses, we next examined its interaction with StSERK3A. TGERa^{LRR9b} and TGERa^{LRR10b} - both unable to bind Pep-13 - exhibited impaired interaction with StSERK3A, consistent with the observation that Pep-13 enhances the interaction between TGERa and StSERK3A. In contrast, Pep-13 failed to induce the interaction between TGERa^{LRR17b} and StSERK3A (Figure 3E). These results demonstrate that TGERb fails to perceive Pep-13 due to defects in both ligand binding and ligand-induced association with StSERK3A.

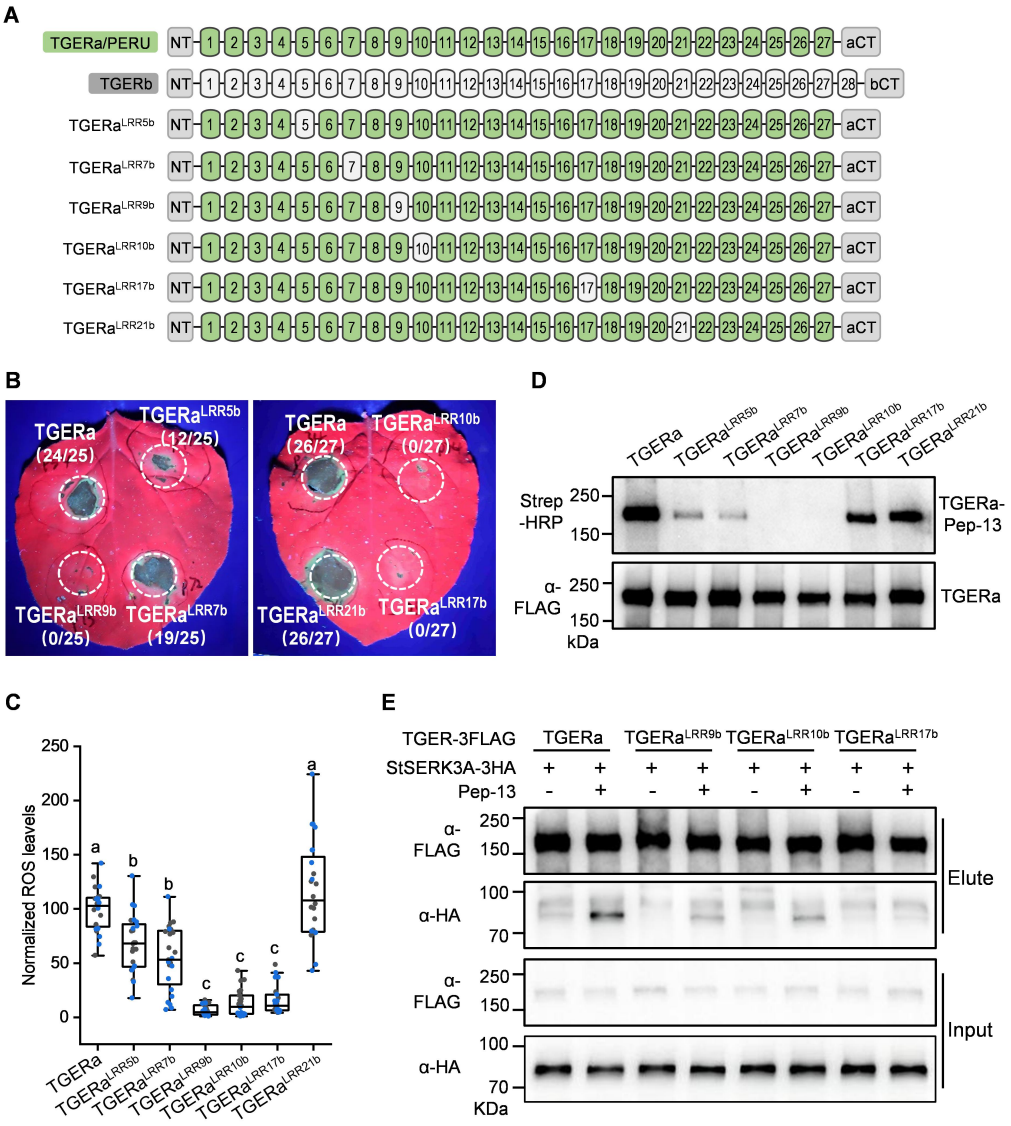

303 **Figure 3. Identification of TGERb's defects in Pep-13 perception.**
304 **(A)** Schematic representation of leucine-rich repeat (LRR) domain swapping between TGERa
305 and TGERb. The ectodomain of TGERa contains 27 LRRs, whereas TGERb has an additional
306 24-amino acid peptide in the region corresponding to LRR24 of TGERa, resulting in 28 LRRs.
307 Indicated LRR regions of TGERb were swapped into the TGERa backbone.
308 **(B-C)** Pep-13-triggered cell death **(B)** and ROS burst **(C)** in *N. benthamiana* (*Nb*) leaves
309 expressing wild-type *TGERa* and chimeric variants carrying the indicated TGERb LRR regions
310 (*TGERa*^{LRRxb}). *TGERa-3Flag* and *TGERa*^{LRRxb}*-3Flag* were transiently expressed in *Nb* leaves
311 for 24 h. For cell death assays, leaves were infiltrated with 100 μM Pep-13, and photos were
312 taken under UV light at 48 h post-infiltration. Numbers in parentheses show the count of
313 necrotic spots versus total spots. For ROS assays, 50 nM Pep-13 was used. The peak value of
314 each ROS curve was normalized to that of TGERa, and analyzed by two-way ANOVA followed
315 by Tukey's multiple comparison test. Different letters indicate significant differences ($p < 0.05$,
316 n = 24 from two independent replicates).
317 **(D)** Differential binding of TGERa and chimeric TGERa^{LRRxb} proteins to biotin-Pep-13.
318 *TGERa-3Flag* and *TGERa*^{LRRxb}*-3Flag* were transiently expressed in *Nb* leaves for 24 h.
319 Leaves were co-infiltrated with 200 nM biotin-Pep-13 and 3 mM EGS, then incubated for 30
320 min at room temperature. Proteins were enriched using M2 beads, and eluates were detected
321 by western blot using anti-Flag antibody and Strep-HRP.
322 **(E)** TGERa, but not TGERa^{LRR17b}, associates with the co-receptor StSERK3A upon Pep-13
323 treatment. *TGERa-3Flag* and *TGERa*^{LRRXb}*-3Flag* was transiently co-expressed with
324 *StSERK3A-3HA* in *Nb* leaves. After 24 h, leaves were infiltrated with 100 μM Pep-13 or H_2O.
325 Samples were collected 15 min post-infiltration, and proteins were enriched using M2 beads.
326 IP eluates were analyzed by western blot using anti-Flag and anti-HA antibodies.
327

328 **TGERa^{A6-10} represents a weak allele with reduced expression levels**

329 To investigate the genetic basis underlying the lack of Pep-13 responsiveness
330 in A6-10, we first examined the genomic organization of TGER loci in diploid
331 potato lines. Using the ePCR function in TBtools-II (Chen et al., 2023b) with
332 TGERa-specific primers, we found that the A6-26 genome contains duplicated
333 TGERa and TGERb loci arranged in a TGERb-TGERa -TGERb-TGERa
334 pattern, which was inherited from its founder line PG6359 (Supplemental Table
335 4). Notably, the CDS of *TGERa*$^{A6-26}$ and *TGERb*$^{A6-26}$ are identical to those of
336 *TGERa*$^{E4-63}$ and *TGERb*$^{E4-63}$, respectively.
337 To identify the corresponding locus in A6-10, we sequenced, assembled, and
338 annotated the A6-10 genome (Supplemental Figure 10; see Supplemental
339 Note 2 for details). The predicted TGERa^{A6-10} protein shares 98.9% amino acid
340 identity with TGERa^{E4-63}. We cloned the CDS of *TGERa*$^{A6-10}$ and transiently

341 expressed in *Nb* leaves. Similar to TGERa^{E4-63}, TGERa^{A6-10} induced MAPK
342 activation and cell death upon Pep-13 treatment (Supplemental Figure 11A
343 and 11B), indicating that the TGERa^{A6-10} protein is functionally intact.
344 Using TBtools-II ePCR, we further identified the *TGERa* genomic sequence in
345 A6-10 genome and detected a ~3-kb insertion within the first intron of
346 *TGERa^{A6-10}* (Supplemental Figure 11C) and this insertion was also present in
347 the founder line PG6359 (Supplemental Table 4), leading us to hypothesize
348 that it might compromise *TGERa* expression in A6-10. Consistent with this
349 hypothesis, transcript analysis revealed that *TGERa* was strongly induced in
350 A6-26 following Pep-13 treatment, whereas only weak induction was observed
351 in A6-10 (Supplemental Figure 11D).
352 Considering that Pep-25 displays stronger cell-death-inducing activity than
353 Pep-13 (Supplemental Figure 3A), we further compared the response of A6-26,
354 A6-10, and Atlantic to both Pep-13 and Pep-25. As shown in Supplemental
355 Figure 11E and 11F, A6-26 exhibited robust cell death as early as 1 day after
356 infiltration with either Pep-25 or Pep-13. In contrast, Pep-25 triggered delayed
357 cell death in A6-10 2-3 days post treatment, whereas Pep-13 failed to induce
358 visible cell death. Neither peptide elicited cell death in Atlantic. Collectively,
359 these results demonstrate that *TGERa^{A6-10}* represents a weak allele
360 characterized by diminished expression, most likely caused by the ~3-kb
361 insertion in its first intron.
362
363 **TGERa improves plant resistance to *Phytophthora* pathogens**
364 To assess the role of TGERa in resistance to *Phytophthora* pathogens,
365 detached leaves of *N. benthamiana* transiently expressing empty vector (EV),
366 *35S:TGERa*, or *35S:TGERb* were inoculated with *P. capsici* BYA5 and
367 incubated in the dark at 28 °C for 2 days; disease progression was then
368 imaged under UV light (Figure 4A). Quantification of diseased leaf areas
369 revealed that TGERa significantly enhanced resistance to *P. capsici* BYA5
370 compared with EV, whereas TGERb did not confer any detectable

371 improvement in disease resistance (Figure 4B).

372

373 To further confirm TGERa conferred enhanced *Phytophthora* resistance, we
374 challenged transgenic *np-TGERa N. benthamiana* lines with *P. infestans* 1306.
375 Detached leaves from *np-TGERa Nb* lines (#1, #2, #3) and wild-type *Nb* plants
376 were inoculated with *P. infestans* and incubated in the dark at 18 °C.
377 Quantification of diseased areas showed significantly smaller lesions in
378 *np-TGERa* lines than in WT (Figures 4C and 4D). Similarly, transgenic
379 *np-TGERa* MicroTom plants exhibited significantly reduced disease symptoms
380 relative to wild-type MicroTom at 2 days post-inoculation (Figures 4E and 4F).
381 Collectively, these results demonstrated that introduction of *TGERa* into
382 heterologous plant species significantly enhances resistance to *Phytophthora*
383 pathogens.

384

385 In summary, using diploid potato inbred lines, we identified TGERa—an allelic
386 variant of PERU—as the receptor for the Phytophthora PAMP Pep-13, and
387 confirmed it mediates Pep-13 perception by forming a receptor complex with
388 SERK family proteins. TGERb, a highly homologous paralog of TGERa, fails to
389 recognize Pep-13 due to ectodomain LRR variations causing defects in both
390 ligand binding and co-receptor association. Meanwhile, the TGERa allele in
391 inbred line A6-10 is a weak variant with reduced expression; though the
392 encoded protein is functionally intact, this low expression results in no visible
393 response to Pep-13 and only delayed cell death upon treatment with the more
394 bioactive Pep-25. We further clarified that TGERa translation initiates at its
395 main ATG codon, that the TGERa isoform derived from intron 2 retention is
396 non-functional, and that the extra amino acid sequence in the annotated
397 $PERU^{LPH}$ is likely an annotation error rather than a determinant of broad ligand
398 recognition. Most importantly, heterologous expression of *TGERa* in *Nicotiana*
399 *benthamiana* and tomato significantly enhanced resistance to *Phytophthora*

infestans, rendering *TGERa* a valuable candidate gene for potato late blight resistance breeding and a novel molecular strategy for improving *Phytophthora* resistance in other crop species.

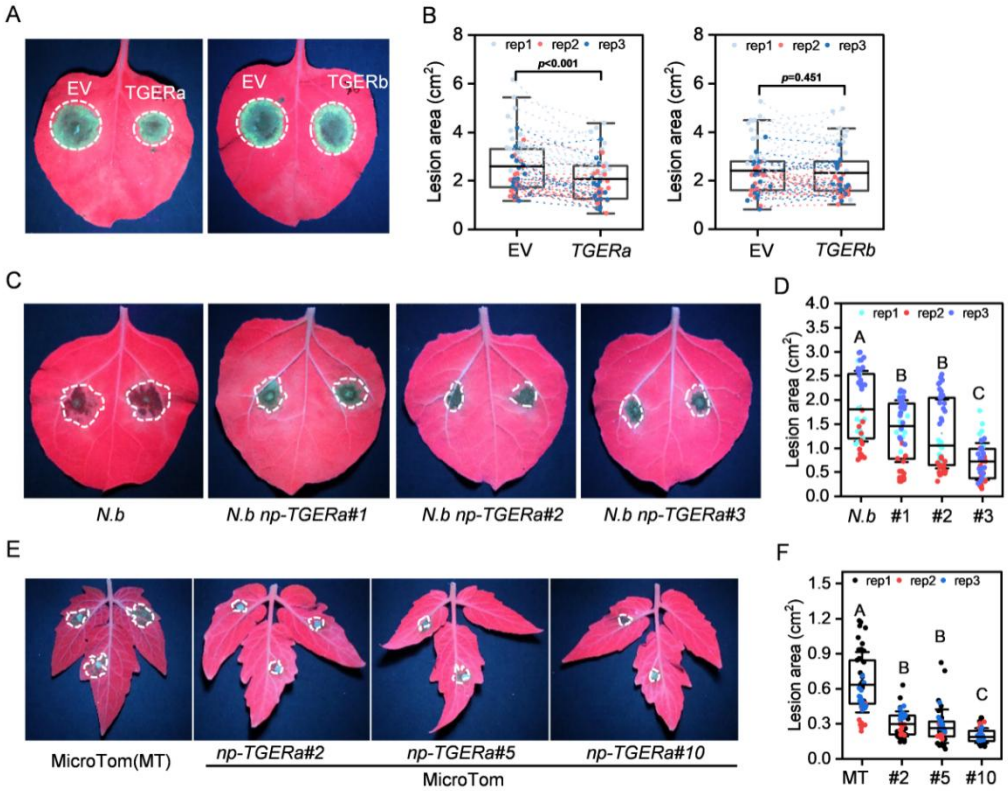

Figure 4. *TGERa* improves plant resistance to *Phytophthora*.

(A-B) *TGERa* enhances resistance to *Phytophthora capsici* when transiently expressed in *N. benthamiana* (*Nb*) leaves. **(A)** Empty vector (EV), *35S-TGERa* and *35S-TGERb* were transiently expressed in *Nb* leaves for 24 h, followed by inoculation with an agar plug (5 mm diameter from colony margins of *P. capsici* strain BYA5. Detached leaves were incubated in the dark at 28°C for 2 days, and lesions were photographed under UV light. **(B)** Quantification of lesion areas using ImageJ. Data were analysed using paired t-test (*TGERa*, $p < 0.05$, n=55 from three independent experiments; *TGERb*, $p = 0.451$, n = 56 from three independent experiments).

(C-D) Transgenic *Nb* lines expressing *TGERa* exhibit enhanced resistance to *P. infestans.* **(C)** Detached leaves of transgenic *Nb* lines (*np-TGERa* #1, *np-TGERa* #2, *np-TGERa* #3) and wild-type *Nb* plants were inoculated with *a* spore suspension of *P. infestans* strain 1306 and incubated in the dark at 18°C for 5 days and photographed under UV light. **(D)** Quantification of lesion areas using ImageJ. Data were analyzed using one-way ANOVA followed by Tukey's test. Different letters indicate significant differences ($p < 0.05$, n = 46 from three independent experiments).

(E-F) Transgenic tomato (MicroTom) lines expressing *TGERa* display enhanced resistance to *P. infestans.* **(E)** Detached leaves were inoculated with a spore suspension of *P. infestans* strain 1306, and lesion sizes were visualized 2 days post-inoculation under UV light. **(F)** Quantification of lesion areas using ImageJ. Data were analyzed using one-way ANOVA

424 followed by Tukey's test. Different letters indicate significant differences ($p < 0.05$, n = 45 from
425 three independent experiments).
426

427 **METHODS**

428 **Plant materials and growth conditions**

429 The diploid potato inbred lines A6-10, E4-63, and A6-26 was previously
430 reported (Zhang et al., 2021). Potato plants and transgenic lines were
431 propagated on Murashige and Skoog (MS) medium in growth chambers under
432 long-day conditions (16 h light at 23°C and 8 h dark at 22°C).
433 For genetic analysis, the Pep-13–insensitive line A6-10 (female parent) was
434 artificially cross-pollinated with E4-63 (male parent) at anthesis to genetate F_1
435 hybrid progeny. The F_1 plants were subsequently self-pollinated to produce the
436 F_2 population. For soil-grown seedlings, *in vitro*-cultured potato plants were
437 grown on MS medium for 1 week then transferred to sterile soil and further
438 cultivated for 14 days. *N. benthamiana* and *S. lycopersicum* MicroTom were
439 directly seed-sown in soil composed of nutrient soil, vermiculite, and perlite
440 (3:2:1, v/v/v). Plants were grown in a growth chamber under long-day
441 conditions (16 h light at 23°C and 8 h dark at 22°C).

442 **Peptide treatments**

443 Peptides Pep-13 (VWNQPVRGFKVYE), Pep-13W2A (VANQPVRGFKVYE),
444 and Pep-25 (DVTAGAEVWNQPVRGFKVYEQTKMS) (Brunner et al., 2002),
445 Biotin-Pep-13, Biotin-Pep-25 and flg22 (QRLSTGSRINSAKDDAAGLQIA)
446 were synthesized by Sangon Biotech (Shanghai, China) Peptides were
447 dissolved in sterile double-distilled water (ddH_2O) to generate 2 mM stock
448 solutions and stored at -20°C. Working solutions were prepared by diluting
449 stock solutions with sterile water to indicated concentrations.

450 **Vector construction**

451 Primers used in this study are listed in Supplemental Table 6. Full-length
452 coding sequences of *TGERa*, *TGERb*, *StSERK1a*, *StSERK1b*, *StSERK2a*,
453 *StSERK2b*, *StSERK3a*, *StSERK3b* were cloned from cDNA library derived

454 from of E4-63 leaf. Domain swapping constructs between TGERa and TGERb
455 LRR regions were generated using gene-specific primers. PCR fragments
456 were inserted into pTF101-35S-3Flag vector (Bu et al., 2021) digested with
457 *XbaI* and *MluI* using homologous recombination. *StSERK1a*, *StSERK1b*,
458 *StSERK2a*, *StSERK2b*, *StSERK3a*, *StSERK3b* were inserted into
459 pCAMBIA1300-35S-3HA vector digested with HindIII and KpnI using
460 homologous recombination.
461 For virus-induced gene silencing constructs, TRV2-NbSERK conserved
462 regions (300-500 bp) within *SERK* coding sequences were identified by
463 BLAST analysis against the tobacco genome. Targeted fragments were
464 amplified and inserted into the TRV2 vector via homologous recombination. All
465 constructs were verified by Sanger sequencing.

466 ***Agrobacterium*-mediated transient expression**

467 Recombinant *Agrobacterium tumefaciens* strains GV3101 harboring the
468 indicated constructs were cultured overnight in LB medium supplemented with
469 kanamycin (50 μg/mL), rifampicin (25 μg/mL), and gentamycin (50 μg/mL) at
470 28 ℃ with shaking at 200 rpm. Bacterial cells were harvested by centrifuged at
471 5000 rpm for 5 min and washed twice with infiltration buffer conting10 mM
472 $MgCl_2$, 10 mM MES (pH 5.6), and 200 μM acetosyringone. Cells were
473 resuspended in infiltration buffer to a final OD_{600} of 0.6 and incubated at room
474 temperature in the dark for 3 h. Fully expanded leaves of 4–5-week-old *N.*
475 *benthamiana* plants were infiltrated on the abaxial side using a needleless
476 syringe. Plants were maintained under low light conditions for 24 h and then
477 returned to normal growth conditions. Protein expression was verified by
478 immunoblot analysis 24-48 h after infiltration. For elicitor assays, infiltration
479 sites were treated with 100 μM Pep-13 at 24 h post infiltration. Hypersensitive
480 cell death was evaluated 48 h later under 365 nm UV light.

481 **RNA isolation and RT-qPCR**

482 RNA isolation and RT-qPCR was performed as described (Chen et al., 2024).
483 *NbEF1α* was used as the reference gene for *N. benthamiana* samples, and

484 *StTUB* was used as the reference gene for potato (*S. tuberosum*). Relative
485 expression levels were calculated using the $2^{-\Delta\Delta CT}$ method. Primer sequences
486 are listed in Supplemental Table 6.

487 **MAPK activation assays**

488 Leaves of potato lines A6-10 and A6-26 were sprayed with 100 μM Pep-13, 5
489 μM flg22 or H_2O. Samples were collected at 15 and 30 min after treatment. *N.*
490 *benthamiana* leaves infiltrated with recombinant *Agrobacterium tumefaciens*
491 GV3101 as described previously for 24 hours, then infiltrated with 50 uM
492 peptides (Pep-13, Pep-25, W2A) for 15 min. Proteins were separated on 10%
493 SDS-PAGE and detected using anti-p44/42-ERK antibody (Cell Signaling
494 #9101).

495 **Virus-induced gene silencing (VIGS)**

496 Cotyledons of 2-week-old *N. benthamiana* plants or transgenic *np-TGERa*
497 lines were infiltrated with a 1:1 mixture of *Agrobacterium* cultures containing
498 pTRV1 and pTRV2 derivatives, *pTRV2-NbPDS*, *TRV2-GFP*, and
499 *pTRV2-NbSERKs* (Wang et al., 2018) adjusted to OD_{600} = 0.5. Two weeks
500 post-infiltration, plants showing photobleaching in *pTRV2-NbPDS*. Gene
501 silencing efficiency was confirmed by RT-qPCR. Leaves were then treated with
502 100 μM Pep-25 or H_2O and cell death responses were documented under 365
503 nm UV light 48 h later.

504 **Electrolyte leakage assay**

505 Electrolyte leakage assay was performed as reported (Fan et al., 2026). Briefly,
506 leaf discs (8 mm) were punched from peptide- or water-infiltrated leaves. Six
507 discs per replicate immersed in 2 mL deionized water. After 3 h incubation at
508 25 °C, initial conductivity (R1) was measured. Samples were boiled for 30 min,
509 cooled to 25 °C, and final conductivity (R2) recorded. Relative electrolyte
510 leakage (REL) was calculated as: REL (%) = (R1/R2) × 100%.

511 **Stable transformation of *N. benthamiana*, *Solanum tuberosum* (*cv.***
512 **Atlantic) and *S. lycopersicum* (*cv.* MicroTom)**

513 Stable transformation of *N. benthamiana*, MicroTom and Atlantic plants was

514 carried out by the BioRun company via *Agrobacterium*-mediated
515 transformation, using the construct *np-TGERa-3Flag* for *N. benthamiana* and
516 MicroTom, and the construct *35S-TGERa-3HA* for Atlantic. Transgenic plants
517 were screened by PCR using gene-specific primer to confirm the presence of
518 the *TGERa* transgene. TGERa protein levels in positive lines were further
519 verified by Western blot analysis.

520 ***In vivo* ligand binding assays**

521 *Agrobacterium tumefaciens* GV3101 carrying *TGERa-3flag* or *TGERb-3flag*
522 constructs was transiently expressed in *N. benthamiana* leaves for 24 h.
523 Leaves were then infiltrated with solutions containing 100 nM biotin–Pep-13/25
524 alone or together with 100 μM unlabeled Pep13/25 as a competition. The
525 infiltration buffer contained 3 mM ethylene glycol bis (succinimidyl succinate)
526 (EGS, Thermo Scientific, #21565) in 25 mM HEPES (pH 7.5). After 30 minutes,
527 approximately 1 g of leaf tissue was harvested and frozen in liquid nitrogen.
528 Proteins were immunoprecipitated using anti-Flag M2 affinity resin
529 (Sigma-Aldrich, A2220-5ML). Bound proteins were analyzed by
530 immunoblotting using anti-Flag antibody (Sigma-Aldrich, F1804-200UG) and
531 streptavidin-HRP (Abcam, Ab7403) to detect receptor-bound biotinylated
532 peptides.

533 **Co-immunoprecipitation assay**

534 Frozen leaf tissue was ground into a fine powder in liquid nitrogen and
535 homogenized in membrane extract buffer containing 25 mM Tris HCl (pH 7.5),
536 10% Glycerol, 1 mM EDTA, 150 mM NaCl, 1.5% NP-40, 0.5% sodium
537 deoxycholate, 1 mM NaF, 4 mM DTT, 2% (w/v) PVPP, 1 mM PMSF, and
538 protease cocktail. Protein extracts were incubated on ice for 30 min and
539 centrifuged at 13,000 × g for 15 min at 4 °C. The supernatants were clarified by
540 a second centrifugation under the same conditions. For immunoprecipitation,
541 the supernatants were incubated with 15 μL anti-FLAG M2 affinity resin
542 (Sigma-Aldrich, A2220-5ML) for 2 h at 4 °C with gentle rotation. Input samples

543 were retained for immunoblot analysis. The resin was washed three times with
544 binding buffer containing 25 mM Tris HCl (pH 7.5), 10% Glycerol, 1 mM EDTA,
545 150 mM NaCl, 1.5% NP-40, 0.5% sodium deoxycholate, 1 mM NaF, 0.2 mM
546 DTT. Bound proteins were eluted by boiling in 2× SDS loading buffer at 95 °C
547 for 5 min. Proteins were separated by SDS–PAGE and detected by
548 immunoblotting using anti-Flag and anti-HA antibodies.

549 **Interacting proteins identified by Immunoprecipitation-Mass**
550 **Spectrometry（IP-MS）**

551 *TGERa-3Flag* or empty vector (EV) constructs were transiently expressed in *N.*
552 *benthamiana* leaves. At 48 h after agroinfiltration, leaves were treated with 100
553 μM Pep-13 or H_2O and harvested 15 min after treatment. Total proteins were
554 extracted and subjected to immunoprecipitation using anti-FLAG M2 affinity
555 resin as described above. Immunoprecipitated proteins were separated by
556 SDS-PAGE and visualized by Coomassie Brilliant Blue staining. Gel regions
557 containing TGERa protein complex were excised and subjected to in-gel
558 digestion with tryptic.
559 The resulting peptides were analyzed by liquid chromatography-tandem mass
560 spectrometry (LC-MS/MS) using an EASY-nLC 1200 system coupled to an
561 Orbitrap Exploris 480 mass spectrometer (Thermo Fisher Scientific). Peptides
562 were separated on a C18 analytical column using a linear acetonitrile gradient.
563 Raw MS data were processed using Proteome Discoverer software and
564 searched against the NbHZ1 protein database (Wang et al., 2024).
565 Carbamidomethylation of cysteine residues was set as a fixed modification,
566 whereas methionine oxidation was considered a variable modification. Up to
567 two missed trypsin cleavage sites were allowed. Peptide spectrum matches
568 were filtered using a false discovery rate (FDR) threshold of <1%. Functional
569 annotation of identified proteins was performed using Gene Ontology (GO),
570 InterPro, COG, and KEGG databases. Only proteins identified in at least two
571 biological replicates were considered for further analysis.

572 **Luminol-based ROS burst assay**

573 Leaf discs (4 mm diameter) were excised from 5-week-old *N. benthamiana*
574 plants were equilibrated overnight in 200 μL ddH_2O in 96-well white plates. The
575 next day, water was replaced with 100 μL reaction buffer containing 10 μg/mL
576 horseradish peroxidase (HRP; Sigma #P6782), 50 μM luminol (Sigma #A8511),
577 and 50 nM Pep-13. Real-time luminescence was recorded at 1 min intervals
578 for 120 min using a Cytation5 microplate reader (BioTek, Winooski, VT, USA)
579 with the following parameters: gain 130, 5 mm read height, no optical filter, and
580 maintaining a constant temperature of 22 °C.

581 **Pathogen infection assay**

582 Infection assays were performed as described previously (Chen et al., 2024). *P.*
583 *infestans* strain 1306 was cultured on rye agar medium at 18 ℃ in darkness for
584 14 days. Zoospores were released by incubating sporangia in cold water at
585 4 °C for 2 h and filtered to remove mycelium. Detached leaves were inoculated
586 with 5 μL zoospore suspension (1×10^5 spores/mL) on the abaxial surface.
587 For *P. capsica* strain BYA5 (Gao et al., 2023), clones were cultured on V8 juice
588 agar medium at 25 ℃ in darkness for 3 days. Agar plugs (5 mm diameter) from
589 colony margins were placed onto leaf surface and covered with 10 μL sterile
590 water. Infected leaves were incubated under 100% relative humidity at optimal
591 temperatures (18 °C for *P. infestans*, 25 °C for *P. capsica*) for 4 or 3 days,
592 respectively. Lesion areas were visualized under UV light and quantified using
593 ImageJ (v1.51j8, National Institutes of Health, Maryland, USA) software.

594 **Statistical Analysis**

595 All experiments were performed with at least three independent biological
596 replicates unless otherwise stated. Data are presented as mean ± standard
597 deviation (SD). Statistical analyses were performed using OriginPro2025
598 (OriginLab). Statistical significance between two groups was determined using
599 a two-tailed Student's t-test, while comparisons among multiple groups were
600 analyzed using one-way analysis of variance (ANOVA) followed by Tukey's
601 multiple comparison test. Differences were considered statistically significant

602 at $p < 0.05$.

603 **DATA AVAILABILITY**

604 The authors hereby declare that all relevant data supporting the findings of this
605 study are accessible within the research article and its supplemental
606 information. The A6-10 genome data has been deposited at
607 http://solomics.agis.org.cn/potato/species, under Accession A6-10 (A6-10).
608 Materials generated during the current study are available from the
609 corresponding author upon reasonable request.

610 **SUPPLEMENTAL INFORMATION**

611 Supplemental information, including Supplemental notes, figures and tables, is
612 available online.

613 Supplemental Note 1. Mapping the TGER locus by BSA-seq analysis.
614 Supplemental Note 2. A6-10 genome assembly and annotation.
615 Supplemental Figure 1. Mapping of *TGER* locus using bulked segregant
616 analysis sequencing
617 Supplemental Figure 2. Transient expression of selected candidate genes in *N.*
618 *benthamiana* leaves by *Agrobacterium* and tested for responding to Pep-13.
619 Supplemental Figure 3. Functional confirmation of TGERa by transgenic
620 complementation.
621 Supplemental Figure 4. Identification of six NbSERK proteins as Pep-13
622 induced interacting proteins of TGERa by IP-MS and phylogenetic analysis of
623 SERK proteins.
624 Supplemental Figure 5. TGERa relies on SERKs for Pep-13 perception.
625 Supplemental Figure 6. Translation initiation from uORF1 of TGERa mRNA
626 leads to decreased TGERa protein levels.
627 Supplemental Figure 7. Intron 2 retention is observed in a subset of
628 TGERa/PERU transcripts.
629 Supplemental Figure 8. The TGERa protein (TGERa-In2R) translated from
630 TGERa mRNA with intron 2 retention cannot recognize Pep-13/25.
631 Supplemental Figure 9. Functional characterization of TGERb in Pep-13
632 perception and signaling.
633 Supplemental Figure 10. Genome assembly and annotation of potato inbred
634 line A6-10.
635 Supplemental Figure 11. TGERa in A6-10 is a weak allele with reduced
636 expression.
637 Supplemental Table 1. 1,981 candidate variants on Chr03 of E4-63 genome
638 identified by BSA-seq analysis.
639 Supplemental Table 2. SNPs identified in selected 24 candidate genes.
640 Supplemental Table 3. Selected candidate genes and cloning primers used.

641 Supplemental Table 4. ipTM between Pep-13 and ectodomains of TGERa,
642 TGERb and TGERa variants predicted using AlphaFold3.
643 Supplemental Table 5. ePCR results for TGER primers in genomes of A6-10,
644 A6-26, E4-63, E86-69, PG6359, DM and Atlantic.
645 Supplemental Table 6. Primers used in this study.
646

647 **FUNDING**

648 The research was supported by grants from the AGIS Talents Start-up
649 Research Fund, Agricultural Science and Technology Innovation Program,
650 Guangdong Basic and Applied Basic Research Foundation
651 (2024A1515010069), and National Natural Science Foundation of China
652 (General Program, 32472579) to TS.
653

654 **AUTHOR CONTRIBUTIONS**

655 T.S., X.F.,and D.L. conceived and designed this study; X.F., D.L., Y.Z., and Y.H.
656 performed the experiments; L.C. analyzed BSA-seq data and performed
657 assembly and annotation of the A6-10 genome. T.S., X.F., and L.C. wrote the
658 manuscript from the input from all other authors. All authors reviewed the
659 manuscript.

660 **ACKNOWLEDGMENTS**

661 We are grateful to Sanwen Huang and Chunzhi Zhang for the potato inbred
662 lines. We kindly thank Yan Wang for pTRV2-NbSERKs, and Fanjiang Kong for
663 pTF101-35S-3FLAG. We also acknowledge Xili Liu for sharing the
664 *Phytophthora capsici* strain BYA5 and the pMDC vector. The authors declare
665 no conflicts of interest.

666 **REFERENCES**

667 **Albert, I., Böhm, H., Albert, M., Feiler, C. E., Imkampe, J., Wallmeroth, N., Brancato, C.,**
668 **Raaymakers, T. M., Oome, S., Zhang, H., et al.** (2015). An RLP23-SOBIR1-BAK1
669 complex mediates NLP-triggered immunity. *Nat. Plants* **1**:1–9.

670 **Brunner, Â., Rosahl, S., Lee, J., Rudd, J. J., Geiler, C., Scheel, D., and Nu, T.** (2002).
671 Pep-13, a plant defense-inducing pathogen-associated pattern from phytophthora

672 transglutaminases. *EMBO J.* **21**:6681–6688.

673 **Bu, T., Lu, S., Wang, K., Dong, L., Li, S., Xie, Q., Xu, X., Cheng, Q., Chen, L., Fang, C., et**
674 **al.** (2021). A critical role of the soybean evening complex in the control of photoperiod
675 sensitivity and adaptation. *Proc. Natl. Acad. Sci. U. S. A.* **118**:1–10.

676 **Chen, Z., Liu, F., Zeng, M., Wang, L., Liu, H., Sun, Y., Wang, L., Zhang, Z., Chen, Z., Xu, Y.,**
677 **et al.** (2023a). Convergent evolution of immune receptors underpins distinct elicitin
678 recognition in closely related Solanaceous plants. *Plant Cell* Advance Access published
679 2023, doi:10.1093/plcell/koad002.

680 **Chen, C., Wu, Y., Li, J., Wang, X., Zeng, Z., Xu, J., Liu, Y., Feng, J., Chen, H., He, Y., et al.**
681 (2023b). TBtools-II: A "one for all, all for one" bioinformatics platform for biological
682 big-data mining. *Mol. Plant* Advance Access published 2023,
683 doi:10.1016/j.molp.2023.09.010.

684 **Chen, Y., Han, Y., Huang, W., Zhang, Y., Chen, X., Li, D., Hong, Y., Gao, H., Zhang, K.,**
685 **Zhang, Y., et al.** (2024). LAZARUS 1 functions as a positive regulator of plant immunity
686 and systemic acquired resistance. *Front. Plant Sci.* **15**:1–11.

687 **Cheng, L., Wang, N., Bao, Z., Zhou, Q., Guarracino, A., Yang, Y., Wang, P., Zhang, Z.,**
688 **Tang, D., Zhang, P., et al.** (2025). Leveraging a phased pangenome for haplotype
689 design of hybrid potato. *Nature* **640**:408–417.

690 **Du, J., Verzaux, E., Chaparro-Garcia, A., Bijsterbosch, G., Keizer, L. C. P., Zhou, J.,**
691 **Liebrand, T. W. H., Xie, C., Govers, F., Robatzek, S., et al.** (2015). Elicitin recognition
692 confers enhanced resistance to Phytophthora infestans in potato. *Nat. Plants* **1**:15034.

693 **Fan, X., Han, Y., Sun, X., and Sun, T.** (2026). Identification and Functional Analysis of Potato
694 Receptor Kinase RDA2 Proteins. *Plants* **15：1-14**.

695 **Gao, H., Guo, Y., Ren, M., Tang, L., Gao, W., Tian, S., Shao, G., Peng, Q., Gu, B., Miao, J.,**
696 **et al.** (2023). Phytophthora RxLR effector PcSnel4B promotes degradation of resistance
697 protein AtRPS2. *Plant Physiol.* **193**:1547–1560.

698 **Jones, J. D., and Dangl, J. L.** (2006). The plant immune system. *Nature* **444**:323–329.

699 **Li, Y., Tao, Y., Yao, X., Cao, R., Xiong, X., Gong, B.-Q., and Li, J.-F.** (2025). SERK5
700 genetically compensates for the loss of BAK1 and BKK1 in regulating elf18-triggered
701 immune signaling in *Arabidopsis*. *Proc. Natl. Acad. Sci.* **122**:e2513517122.

702 **Ma, X., Xu, G., He, P., and Shan, L.** (2016). SERKing Coreceptors for Receptors. *Trends*
703 *Plant Sci.* **21**:1017–1033.
704 **Nietzschmann, L., Gorzolka, K., Smolka, U., Matern, A., Eschen-Lippold, L., Scheel, D.,**
705 **and Rosahl, S.** (2019). Early Pep-13-induced immune responses are
706 SERK3A/B-dependent in potato. *Sci. Rep.* **9**:1–12.
707 **Nowicki, M., Foolad, M. R., Nowakowska, M., and Kozik, E. U.** (2012). Potato and Tomato
708 Late Blight Caused by Phytophthora infestans : An Overview of Pathology and
709 Resistance Breeding. *Plant Dis.* **96**:4–17.
710 **Nürnberger, T., Nennstiel, D., Jabs, T., Sacks, W. R., Hahlbrock, K., and Scheel, D.** (1994).
711 High affinity binding of a fungal oligopeptide elicitor to parsley plasma membranes
712 triggers multiple defense responses. *Cell* **78**:449–460.
713 **Stokstad, E.** (2019). The new potato. *Science (80-.).* **363**:574–577.
714 **Torres Ascurra, Y. C., Zhang, L., Toghani, A., Hua, C., Rangegowda, N. J., Posbeyikian,**
715 **A., Pai, H., Lin, X., Wolters, P. J., Wouters, D., et al.** (2023). Functional diversification
716 of a wild potato immune receptor at its center of origin. *Science (80-.).* **381**:891–897.
717 **Wang, Y., Xu, Y., Sun, Y., Wang, H., Qi, J., Wan, B., Ye, W., Lin, Y., Shao, Y., Dong, S., et**
718 **al.** (2018). Leucine-rich repeat receptor-like gene screen reveals that Nicotiana RXEG1
719 regulates glycoside hydrolase 12 MAMP detection. *Nat. Commun.* **9**.
720 **Wang, J., Zhang, Q., Tung, J., Zhang, X., Liu, D., Deng, Y., Tian, Z., Chen, H., Wang, T.,**
721 **Yin, W., et al.** (2024). High-quality assembled and annotated genomes of Nicotiana
722 tabacum and Nicotiana benthamiana reveal chromosome evolution and changes in
723 defense arsenals. *Mol. Plant* **17**:423–437.
724 **Zhang, C., Yang, Z., Tang, D., Zhu, Y., Wang, P., Li, D., Zhu, G., Xiong, X., Shang, Y., Li,**
725 **C., et al.** (2021). Genome design of hybrid potato. *Cell* **184**:3873-3883.e12.
726 **Zhou, J., and Zhang, Y.** (2020). Plant Immunity: Danger Perception and Signaling. *Cell*
727 **181**:978–989.
728